Published in final edited form as:
Nat Struct Mol Biol. 2014 February ; 21(2): 175–179. doi:10.1038/nsmb.2753.

RNA polymerase II termination involves CTD tyrosine dephosphorylation by CPF subunit Glc7

Amelie Schreieck[#1], **Ashley D. Easter**[#2], **Stefanie Etzold**[1], **Katrin Wiederhold**[2], **Michael Lidschreiber**[1], **Patrick Cramer**[1], and **Lori A. Passmore**[2]

[1]Gene Center Munich and Department of Biochemistry, Center for Integrated Protein Science Munich (CIPSM), Ludwig-Maximilians-Universität München, Munich, Germany.

[2]Medical Research Council (MRC) Laboratory of Molecular Biology, Cambridge, United Kingdom.

[#] These authors contributed equally to this work.

Abstract

At the 3′ end of protein-coding genes, RNA polymerase (Pol) II is dephosphorylated at tyrosine (Tyr1) residues of its C-terminal domain (CTD). In addition, the associated cleavage and polyadenylation (pA) factor (CPF) cleaves the transcript and adds a polyA tail. Whether these events are coordinated and how they lead to transcription termination remains poorly understood. Here we show that CPF from *Saccharomyces cerevisiae* is a Pol II CTD phosphatase and that the CPF subunit Glc7 dephosphorylates Tyr1 *in vitro*. *In vivo*, the activity of Glc7 is required for normal Tyr1 dephosphorylation at the pA site, for recruitment of termination factors Pcf11 and Rtt103, and for normal Pol II termination. These results show that transcription termination involves Tyr1 dephosphorylation of the CTD and indicate that pre-mRNA processing by CPF and transcription termination are coupled via Glc7-dependent Pol II Tyr1 dephosphorylation.

The synthesis of mRNA by Pol II involves co-transcriptional pre-mRNA processing including 5′-capping, splicing and 3′-end processing. Pol II recruits pre-mRNA processing factors via its CTD throughout transcription[1-3] and this process is regulated by changes in CTD phosphorylation[4]. The CTD forms a flexible extension of Pol II consisting of 26 (yeast) or 52 (human) heptapeptide repeats of the consensus sequence Tyr1–Ser2–Pro3–Thr4–Ser5–Pro6–Ser7. When Pol II is recruited to promoters, the CTD is not phosphorylated[4]. As transcription proceeds, Ser5 phosphorylation recruits the mRNA 5′-capping machinery near the promoter[5,6], whereas Ser2 phosphorylation recruits 3′-processing and termination factors near the pA site[7]. Tyr1 phosphorylation prevents premature recruitment of termination factors within gene bodies[8]. At the pA site, Tyr1 phosphorylation levels drop, whereas Ser2 phosphorylation remains, apparently enabling

Correspondence and requests for materials should be addressed to LAP (passmore@mrc-lmb.cam.ac.uk) and PC (cramer@LMB.uni-muenchen.de)..

Author Contributions AS, ADE, SE, and KW performed experiments. ML analyzed data. LAP and PC designed and supervised research. AS, ADE, LAP, and PC wrote the manuscript.

Accession codes Raw and normalized ChIP-chip data are available at ArrayExpress (http://www.ebi.ac.uk/arrayexpress/) under accession number E-MTAB-1528.

Author Information Reprints and permissions information is available at www.nature.com/reprintsandpermissions.

The authors declare no competing financial interests.

Supplementary methods and any associated references are available in the **Supplementary Information** linked to the online version of the paper at www.nature.com/nsmb.

Europe PMC Funders Author Manuscripts

termination factor recruitment[8]. Thus, CTD kinases and phosphatases play key roles in mRNA synthesis[4].

Addition of a 3′ polyA tail to mRNA facilitates nuclear export, regulates the stability of mRNAs and enhances translation[9-11]. 3′-end processing is performed by a large number of proteins including the ~1 MDa CPF complex (CPSF in mammals), which cleaves pre-mRNA with its endonuclease subunit (Ysh1/CPSF73) and then polyadenylates the new 3′-end with its polyA polymerase (Pap1/PAP)[12, 13]. Accessory proteins, such as CF IA (comprised of Pcf11, Clp1, Rna14 and Rna15) and CF IB in yeast, contribute to the specificity and efficiency of 3′-end processing reactions.

The cleavage and polyadenylation machinery is recruited to nascent transcripts early in the transcription cycle. CPF associates with the Pol II CTD and TFIID at promoters and is presumed to travel with the transcription complex until it reaches the pA site[12]. Interestingly, the Pol II CTD itself is proposed to play a role in 3′-end processing since it is required for efficient pre-mRNA processing *in vivo*[14,15] and stimulates the cleavage event *in vitro*[16]. Disruption of 3′-end processing can lead to defects in transcription termination suggesting an intimate link between these two processes[17]. For example, temperature sensitive mutations in CF IA subunits result in defective transcription termination[18]. Pcf11 contains a CTD-interacting domain (CID) that binds Ser2-phosphorylated CTD and plays a role in transcription termination, separable from its role in 3′-end processing [15,19-21].

The transition from transcription elongation to termination involves CTD Tyr1 dephosphorylation by an unknown phosphatase. We reasoned that the Tyr1 phosphatase might be part of the mRNA 3′-end processing and termination machinery. In particular, CPF contains two candidate phosphatases, Ssu72[22,23] and Glc7[24]. Ssu72 can dephosphorylate CTD residue Ser5 during transcription elongation[22,25,26]. Glc7 is implicated in transcription termination on snoRNA genes[27], in mRNA export[28] and in the polyadenylation activity of CPF[29] but has no known CTD-related activity. We therefore set out to investigate the role of CPF in CTD phosphorylation. Here, we show that Glc7 is a Tyr1 phosphatase both *in vitro* and *in vivo*. We further show that Glc7 is required for normal recruitment of termination factors and Pol II termination *in vivo*.

RESULTS

CPF subunit Glc7 dephosphorylates CTD Tyr1 *in vitro*

To investigate whether Ssu72 or Glc7 has CTD Tyr1 phosphatase activity we purified endogenous CPF from yeast. Analysis of the entire CPF complex was necessary since isolated phosphatases generally have little specificity, and target-specific dephosphorylation often relies on cofactors[30]. The resulting preparations contained all CPF subunits, including Ssu72 and Glc7 (Fig. 1a). To test CPF preparations for CTD phosphatase activity, we used a substrate of purified yeast Pol II that had been pre-phosphorylated with MAP kinase, including on Tyr1, Ser2, and Ser5 (Methods; Fig. 1b, lane 1). In these assays, we used a molar ratio of CPF to Pol II of 1:4, *i.e*. 1:104 of CPF to each Pol II CTD heptad. Incubation with CPF led to almost complete dephosphorylation of Tyr1, Ser2 and Ser5, as revealed by Western blotting (Fig. 1b, lanes 3–5).

To identify which of the two CPF phosphatases was responsible for Tyr1 dephosphorylation, we specifically inhibited Glc7 with EDTA or microcystin. EDTA chelates metal ions and abolishes activity of the metal ion-dependent phosphatase Glc7[31,32], but does not affect Ssu72 activity, which is metal ion-independent[23]. Microcystin is a bacterial toxin that specifically inhibits PP1 and PP2A-type phosphatases[30] including Glc7, but not Ssu72. Addition of 10 mM EDTA or 200 nM microcystin to the reaction selectively inhibited Tyr1

and Ser2 dephosphorylation, whereas Ser5 dephosphorylation was still observed (Fig. 1b, lanes 6–13). These results show that the Glc7 subunit of CPF functions as a CTD phosphatase for Tyr1 and Ser2 *in vitro*.

Glc7 is required for Tyr1 dephosphorylation *in vivo*

To investigate whether Glc7 acts as a CTD phosphatase *in vivo*, we depleted Glc7 from the nucleus using the anchor-away method[33] (Supplementary Fig. 1a) and monitored changes in genome-wide occupancy of Tyr1- and Ser2-phosphorylated Pol II by chromatin immunoprecipitation (ChIP) profiling[34]. For metagene analysis of ChIP-chip data, we aligned genes at their pA sites and excluded genes flanked by a neighboring gene within 400 nucleotides downstream of their pA site. This showed that nuclear depletion of Glc7 with rapamycin led to a defect in Tyr1 dephosphorylation at the pA site (Fig. 2a). In addition, the levels of Tyr1 phosphorylation increased around the transcription start site (TSS, Supplementary Fig. 2). The defect in Tyr1 dephosphorylation was also observed on individual genes (Fig. 2b), and was not due to treatment with rapamycin (Supplementary Fig. 3).

Nuclear depletion of Glc7 specifically affected Tyr1 dephosphorylation, and not Ser2 dephosphorylation. ChIP occupancy of Ser2-phosphorylated Pol II normalized against total Pol II occupancy revealed no changes around the pA site, whereas occupancy with Tyr1-phosphorylated Pol II increased (Fig. 2c,d). Thus the Glc7-dependent Ser2 dephosphorylation observed *in vitro* (Fig. 1b) is likely non-specific and not used *in vivo*, consistent with the previously observed Ser2 dephosphorylation by Fcp1 *in vivo*[25,35].

Although the mammalian homologue of Glc7, protein phosphatase 1 (PP1), acts primarily on phosphorylated serine and threonine residues[30,36], the recombinant enzyme is active on phosphorylated tyrosine residues[37]. Tyrosine dephosphorylation can also be performed by the related *Arabidopsis* PPP-Kelch phosphatase BSU1[38,39] and the serine-threonine protein phosphatase 2A (PP2A) if activated by the correct binding partner[40]. Our results for Glc7 demonstrate that a PP1 enzyme can act on a natural phosphorylated tyrosine substrate when present in the context of the correct multiprotein complex – in this case, CPF.

Ssu72 does not dephosphorylate Tyr1

As previously predicted[22,23], Ssu72 was recently shown to contain a protein tyrosine phosphatase fold[26], but it apparently acts as a serine-specific phosphatase. Indeed, we found that recombinant human Ssu72 was able to dephosphorylate Ser5 but neither Tyr1 nor Ser2 *in vitro*, with up to 1.4 molar excess hSsu72 for each Pol II CTD heptad substrate (Fig. 3a). This is consistent with previous reports that Ssu72 is a CTD Ser5 phosphatase[22,25,26].

To investigate whether indeed Ssu72 does not dephosphorylate Tyr1 *in vivo*, we prepared a Ssu72-FRB anchor-away yeast strain and depleted Ssu72 from the nucleus by rapamycin addition. ChIP-chip experiments after Ssu72 nuclear depletion showed that Tyr1 dephosphorylation at the pA site was not influenced (Fig. 3b), suggesting that Glc7 remained in the nucleus and dephosphorylated Tyr1 normally. To show this, we tagged Glc7 with mCherry in the Ssu72-FRB strain, and found that the localization of Glc7 was not influenced by rapamycin addition (Supplementary Fig. 1). These results are consistent with a previous report that a point mutation in the CPF subunit Ref2 leads to Glc7 dissociation but has no impact on the integrity of the remaining complex[27]. Taken together, these results indicate that Glc7 or Ssu72 can be depleted from CPF without destabilizing the complex, and that Glc7 catalyzes Tyr1 dephosphorylation, whereas Ssu72 does not.

Glc7 is involved in transcription termination

Additional ChIP data indicated that Glc7 is required for transcription termination. The ChIP signal for total Pol II (Rpb3 subunit) normally decreases about 200 nucleotides downstream of the pA site, due to transcription termination and Pol II release from DNA (Fig. 4a, black line). Upon nuclear depletion of Glc7 however, strong Pol II ChIP signals remained further downstream (Fig. 4a, dotted black line). These data suggest that Glc7 acts globally and may be required for normal transcription termination *in vivo*.

To investigate whether Tyr1 dephosphorylation is required for normal termination factor recruitment, we determined Pcf11 and Rtt103 ChIP-chip occupancy after Glc7 nuclear depletion (Fig. 4b). These experiments revealed a strong decrease in termination factor occupancy. Both Pcf11 and Rtt103 showed much lower occupancies downstream of the pA site after rapamycin addition, indicating that the defect in Pol II termination (Fig. 4a) results from a defect in termination factor recruitment.

DISCUSSION

Whereas previous work showed that the Pol II CTD is phosphorylated at Tyr1, and that Tyr1 phosphorylation impairs binding of transcription termination factors[8], it remained unknown whether Tyr1 dephosphorylation is required for termination *in vivo* and which enzyme dephosphorylates Tyr1. Here we establish yeast CPF subunit Glc7 as a CTD Tyr1 phosphatase, and show that Tyr1 dephosphorylation is required for normal recruitment of termination factors and transcription termination. These results support the previously proposed ‘extended CTD code’ for the coordination of factor recruitment during the transcription cycle[8] and indicate a crucial role for Tyr1 dephosphorylation in the elongation-termination transition.

The data presented here and previously[8] lead to the following model for the elongation-termination transition of Pol II at the 3′-ends of protein-coding genes (Fig. 4c). Elongating Pol II is phosphorylated mainly at Tyr1 (Y1P) and Ser2 (S2P), and this facilitates elongation factor binding. Tyr1 phosphorylation impairs premature recruitment of termination factors. When Pol II reaches the pA site, the Glc7 subunit of CPF dephosphorylates Tyr1 (−Y1P), whereas Ser2 phosphorylation levels remain high. This allows for the binding of Pcf11 and Rtt103, termination factors that are not part of CPF and show peak occupancy ~100 nucleotides downstream of the pA site[8]. Both Pcf11 and Rtt103 contain CIDs that interact with Ser2-phosphorylated CTD[19,41]. Further downstream, transcription terminates and Pol II is released from genes. When Glc7 is depleted from the nucleus (+ Rapa), Tyr1 phosphorylation levels remain high downstream of the pA site, impairing termination and Pol II release which causes readthrough. In addition, we observed an influence of Glc7 depletion on Tyr1 phosphorylation levels near the TSS (Supplementary Fig. 2). This may be explained by initiation with polymerases that remained partially phosphorylated on Tyr1 residues, by termination defects at upstream genes[24], or by a possible role of Glc7 in transcription attenuation, which would be consistent with the role of Glc7 in Nrd1-dependent termination of snoRNA genes[27].

Our results also provide evidence that pA-dependent 3′-pre-mRNA processing is coupled to transcription termination via CPF-triggered Pol II dephosphorylation. A link between the pA site and transcription termination was established over 25 years ago[42]. In the ‘anti-terminator’ model, transcription of the pA site triggers a change in the Pol II machinery that allows for termination[1,2,43]. In the ‘torpedo’ model, CPF-dependent RNA cleavage at the pA site results in a new RNA 5′-end that is recognized by the Rat1–Rai1–Rtt103 exonuclease complex, which degrades nascent RNA and triggers termination[1,2,43]. Our data are consistent with a combination of both models; Tyr1 phosphorylation would serve as an anti-

terminator that is removed at the pA site by Glc7, allowing for recruitment of termination factors, including the torpedo nuclease complex that contains Rtt103.

ONLINE METHODS

CPF purification and analysis

Primers specific to 40-bp of the C-terminus and 3′-UTR of *REF2* were used to PCR amplify the TAP tag cassette from a modified pFA6a-TAP-kanMX6 vector[44], where a StrepII tag replaces the calmodulin binding peptide. The PCR product was transformed into *Saccharomyces cerevisiae* strain JWY104 (*MATalpha pra1-1 prb1-1 prc1-1 cps1-3 ura3Δ5 leu2-3 his-*, obtained from S. Munro, MRC LMB) via homologous recombination. Cells were grown at 30 °C in YPD to an $OD_{600\ nm}$ of 5.0-5.5, pelleted at 6700 *g*, washed once with cold water, pelleted at 3200 *g*, snap-frozen in liquid N_2 and stored at −80 °C. Cells were mixed 1:1 v:v with lysis buffer (100 mM Hepes pH 7.9, 200 mM KCl, 0.5 mM $MgCl_2$, 0.5 mM $Mg(OAc)_2$, 10% glycerol, 1.6 μg/mL DNAse I and EDTA-free protease inhibitor cocktails tablets (Roche)) and lysed at 35 kPsi via cell disruption (Constant Systems). Lysate was clarified at 25000 *g* for 25 minutes, bound to IgG sepharose (GE Healthcare) for 1 hour and washed with buffer A (20 mM Hepes pH 7.9, 150 mM KCl, 3 mM DTT, 0.5 mM $MgCl_2$, 0.5 mM $Mg(OAc)_2$, 0.2 mM PMSF and 0.2 mM benzamidine-HCl). CPF was eluted from the IgG resin with TEV protease at 16 °C for 1.5 hours, and the supernatant applied to StrepTactin sepharose (GE Healthcare) for 1 hour. StrepTactin resin was washed 3 times with buffer B (buffer A at 400 mM KCl), 3 times with buffer C (buffer A without PMSF and benzamidine), then eluted with 5 mM desthiobiotin in buffer C. Concentration was determined via absorbance at 280 nm using a calculated extinction coefficient. Bands were excised from Coomassie blue-stained SDS-PAGE gels (Fig. 1a) and identified via tryptic digest mass spectrometry.

Dephosphorylation assay

After prephosphorylation of RNA Pol II[45] with MAP Kinase (P6080S; NEB) for 60 minutes at 30 °C, the kinase was inactivated for 20 minutes at 65 °C, then 234 nM RNA Pol II was incubated with 59 nM CPF at 30 °C for indicated periods in buffer C. For Glc7 inhibition, 10 mM EDTA or 200 nM microcystin-LR (Sigma) was added. Samples were dissolved in 3x SDS-PAGE buffer (250 mM Tris-HCl pH 6.8, 100 mM DTT, 7.5% SDS, 50% glycerol, 0.03% bromophenol blue) and boiled at 95 °C for 90 seconds. After SDS-PAGE (0.5 μg of Pol II per lane), samples were blotted onto a polyvinylidene difluoride (PVDF) membrane (Millipore) and the membrane was probed with primary antibodies anti-Tyr1-P (3D12, dilution 1:7)[8], anti-Ser5-P (3E8, dilution 1:4)[46], anti-Ser2-P (3E10, dilution 1:14)[46], kindly provided by Dirk Eick (Helmholtz-Zentrum München), and anti-Rpb3 (1Y26, cat. no. W0012, neoclone, dilution 1:1000). Secondary antibodies anti-rat IgG HRP (A9037, Sigma, dilution 1:5000) and anti-mouse IgG HRP (170-6516, BioRad, dilution 1:3000) were used. Antibody detection was performed using Pierce enhanced chemiluminescence (ECL) Western blotting substrate (Thermo Scientific) and Amersham Hyperfilm ECL (GE Healthcare) or LAS-3000 camera (FUJIFILM).

For Pol II dephosphorylation with human Ssu72 (hSsu72), the protein was expressed and purified as described[23]. 3 μg of Pol II was incubated with 1, 3 or 5 μg purified recombinant hSsu72 in Ssu72 buffer (50 mM Tris-HCl pH 8.0, 10 mM $MgCl_2$, 20 mM KCl, 2% glycerol, 5 mM DTT, 0.1 mM EDTA, 0.025% Tween 20) for 2 hours at 30°C. Samples were dissolved in 3x SDS-PAGE buffer and processed as described above.

Original images of blots used in this study can be found in Supplementary Fig. 4.

Europe PMC Funders Author Manuscripts

Yeast strains and methods

Yeast strains Glc7-FRB-KanMX6 and Ssu72-FRB-KanMX6 were constructed by amplifying the cassette from vector pFA6a-FRB-KanMX6 (P30578, Euroscarf) with suggested primer pairs and transforming the parental strain HHY168 (Y40343, Euroscarf, *MATα ade2-1 trp1-1 can1-100 leu2-3,112 his3-11,15 ura3 GAL psi+ tor1-1 fpr1::NAT RPL13A-2×FKBP12::TRP1*) by homologous recombination. The mCherrytag on Glc7 in the Ssu72-FRB-KanMX6 strain and the TAP-tags on Pcf11 and Rtt103 in the Glc7-FRB-KanMX6 strain were inserted by homologous recombination of PCR products amplified from the pFA6a-mCherry-His3MX6 and pYM-TAP-HIS3MX6 plasmids, respectively.

For serial dilution growth assays, cells were grown in YPD at 30 °C to stationary phase and resuspended to an $OD_{600\ nm}$ of 1.0 in water. 3 μL of cells were spotted onto YPD, with or without 1 μg/mL rapamycin (Cayman Chemical) in 10-fold serial dilutions. Plates were incubated at 30°C and inspected daily.

For fluorescence microscopy, cells were grown in 1 mL YPD + 40 μg/mL adenine hemisulfate (Sigma) to $OD_{600\ nm}$ ~0.8 and 0.5 mL of paraformaldehyde solution (10% paraformaldehyde (Sigma), 13 mM NaOH, 150 mM PBS) was added for 10 minutes. Cells were washed with PBS once, resuspended in 50 μL PBS and applied to a poly-L-lysine-coated glass slide (Sigma, Roth). Remaining liquid was removed and 1.0 ng/μL DAPI (Sigma) in PBS was applied for 1 minute. Fixed cells on glass slides were washed twice with PBS and covered with a cover slip. DAPI and mCherry fluorescence was analyzed under the microscope (Leica DM2500, EL 6000). Camera DFC365FX and Software LAS AF 6000 Modular Systems Version 2.6.0.7266 (Leica) were used for image analysis.

Chromatin immunoprecipitation

Experiments were performed in duplicates as described elsewhere[47] with the following modifications: Yeast cultures were grown in 400 mL YPD to $OD_{600\ nm}$ ~0.65, split and incubated with equal volumes of either rapamycin (1 μg/mL f.c. in DMSO) or DMSO at 30 °C for another 60 minutes before formaldehyde crosslinking. Precooled lysis buffer additionally contained a phosphatase inhibitor cocktail (PhosSTOP, Roche) when Tyr1-P, Ser2-P or Ser5-P were immunoprecipitated. Cell disruption by bead beating was performed for 2 hours. For immunoprecipitation, 700 μL of chromatin sample was incubated with 16.5 μL antibody-coated and prewashed magnetic Protein G beads (Dynabeads® Protein G, Life Technologies) at 4 °C overnight or for 3 hours when TAP tags were immunoprecipitated. Beads were prewashed 4 times with BSA:PBS (5 mg/mL bovine serum albumin in 137 mM NaCl, 2.7 mM KCl, 8.1 mM $Na_2HPO_4•2H_2O$, 1.4 mM KH_2PO_4 pH 7.4 with protease inhibitors), coated with the respective antibody for 30 minutes at 4 °C (100 μL anti-Tyr1-P (3D12), 25 μL anti-Ser2-P or 5μL anti-Rpb3 (1Y26, cat. no. W0012, neoclone) or 13.6 μg rabbit IgG (SIGMA) for TAP tags per chromatin sample) and washed again 3 times. After immunoprecipitation, beads were washed 5 times with wash buffer (100 mM Tris-HCl pH 7.5, 500 mM LiCl, 1% NP40, 1% sodium deoxycholate) and once with TE buffer (10 mM Tris-HCl pH 7.4, 1 mM EDTA). Immunoprecipitated chromatin was eluted for 5 minutes at 95 °C with ChIP elution buffer (0.1 M $NaHCO_3$, 1% SDS). Eluted chromatin was digested with Proteinase K (Sigma) at 37 °C for 2 hours and the reversal of crosslinks was performed at 65 °C overnight. DNA was purified with the QIAquick PCR Purification Kit (Qiagen) according to the manufacturer's instructions. DNA amplification and labeling as well as microarray handling were performed as described[34].

ChIP-chip occupancy profiling

ChIP-chip data analysis was performed as described[34] with some modifications. Briefly, first we performed quantile normalization between replicate measurements and averaged the

signal for each probe over the replicate intensities for the Glc7-FRB strain. For Supplementary Fig. 3, one replicate was analyzed. ChIP enrichments were obtained by dividing ChIP intensities by the corresponding input intensities. The normalized ChIP signal at each nucleotide was calculated as the median signal for all probes overlapping this position. Profiles were smoothed using running median smoothing with a window half size of 75 bp. To average profiles over genes, yeast genes were filtered: Of 4,366 yeast genes with annotated TSS and pA sites[48], we excluded genes shorter than 800 bp or with a neighbouring gene within 400 bp downstream of the pA site. The resulting 619 genes were aligned at their pA sites and the ChIP signals averaged in a region from 400 bp upstream to 400 bp downstream. Averaging was performed by calculating the median over genes at each genomic position. Since CPF acts around the pA site, we were especially interested in whether the profiles change around the pA site relative to the region upstream of the pA site. To better visualize these relative differences we further normalized the data to have approximately equal occupancy levels upstream (around – 400 bp) of the pA site for the '−' and '+' rapamycin treated profiles. Corresponding non-normalized data averaged over the entire gene length (250 bp upstream of TSS to 400 bp downstream of pA site) are shown in Supplementary Fig. 2.

Changes in termination factor occupancy were visualized over the entire gene length. Therefore genes of medium length (1238 ± 300 bp, n = 339) were aligned at their TSS and pA sites, scaled to median length, and averaged at each genomic position.

Supplementary Material

Refer to Web version on PubMed Central for supplementary material.

Acknowledgments

We thank A. Cheung (Cramer laboratory), N.A. Yewdall (Passmore laboratory) and the mass spectrometry facility at the MRC-LMB for help, D. Barford for discussions, and E. Kremmer and D. Eick (Helmholtz Zentrum München) for antibodies. ADE was supported by a Woolf Fisher Trust Scholarship and KW was supported by a fellowship from the Deutsche Forschungsgemeinschaft. Work in the lab of LAP is supported by Medical Research Council grant MC_U105192715 (LAP) and ERC Starting Grant no. 261151 (LAP). PC was supported by the Deutsche Forschungsgemeinschaft (SFB646, TR5, SFB960, CIPSM, NIM), an ERC Advanced Grant, the Jung-Stiftung and the Vallee Foundation.

REFERENCES

1. Brannan K, Bentley DL. Control of Transcriptional Elongation by RNA Polymerase II: A Retrospective. Genet Res Int. 2012; 2012:170–173. [PubMed: 22567377]
2. Buratowski S. Progression through the RNA polymerase II CTD cycle. Mol. Cell. 2009; 36:541–546. [PubMed: 19941815]
3. Corden JL. Transcription. Seven ups the code. Science. 2007; 318:1735–1736. [PubMed: 18079391]
4. Jeronimo C, Bataille AR, Robert F. The Writers, Readers, and Functions of the RNA Polymerase II C-Terminal Domain Code. Chem. Rev. 2013; 113:8491–8522. [PubMed: 23837720]
5. Komarnitsky P, Cho EJ, Buratowski S. Different phosphorylated forms of RNA polymerase II and associated mRNA processing factors during transcription. Genes Dev. 2000; 14:2452–2460. [PubMed: 11018013]
6. Schroeder SC, Schwer B, Shuman S, Bentley D. Dynamic association of capping enzymes with transcribing RNA polymerase II. Genes Dev. 2000; 14:2435–2440. [PubMed: 11018011]
7. Ahn SH, Kim M, Buratowski S. Phosphorylation of serine 2 within the RNA polymerase II C-terminal domain couples transcription and 3′ end processing. Mol. Cell. 2004; 13:67–76. [PubMed: 14731395]
8. Mayer A, et al. CTD tyrosine phosphorylation impairs termination factor recruitment to RNA polymerase II. Science. 2012; 336:1723–1725. [PubMed: 22745433]

9. Niño CA, Hérissant L, Babour A, Dargemont C. mRNA nuclear export in yeast. Chem. Rev. 2013; 113:8523–8545. [PubMed: 23731471]
10. Garneau NL, Wilusz J, Wilusz CJ. The highways and byways of mRNA decay. Nat. Rev. Mol. Cell Biol. 2007; 8:113–126. [PubMed: 17245413]
11. Kapp LD, Lorsch JR. The molecular mechanics of eukaryotic translation. Annu. Rev. Biochem. 2004; 73:657–704. [PubMed: 15189156]
12. Zhao J, Hyman L, Moore C. Formation of mRNA 3′ ends in eukaryotes: mechanism, regulation, and interrelationships with other steps in mRNA synthesis. Microbiol. Mol. Biol. Rev. 1999; 63:405–445. [PubMed: 10357856]
13. Mandel CR, Bai Y, Tong L. Protein factors in pre-mRNA 3′-end processing. Cell. Mol. Life Sci. 2008; 65:1099–1122. [PubMed: 18158581]
14. McCracken S, et al. The C-terminal domain of RNA polymerase II couples mRNA processing to transcription. Nature. 1997; 385:357–361. [PubMed: 9002523]
15. Licatalosi DD, et al. Functional interaction of yeast pre-mRNA 3′ end processing factors with RNA polymerase II. Mol. Cell. 2002; 9:1101–1111. [PubMed: 12049745]
16. Hirose Y, Manley JL. RNA polymerase II is an essential mRNA polyadenylation factor. Nature. 1998; 395:93–96. [PubMed: 9738505]
17. Proudfoot NJ. Ending the message: poly(A) signals then and now. Genes Dev. 2011; 25:1770–1782. [PubMed: 21896654]
18. Birse CE, Minvielle-Sebastia L, Lee BA, Keller W. Coupling termination of transcription to messenger RNA maturation in yeast. Science. 1998
19. Barillà D, Lee BA, Proudfoot NJ. Cleavage/polyadenylation factor IA associates with the carboxyl-terminal domain of RNA polymerase II in Saccharomyces cerevisiae. Proc. Natl. Acad. Sci. U.S.A. 2001; 98:445–450. [PubMed: 11149954]
20. Sadowski M, Dichtl B, Hübner W, Keller W. Independent functions of yeast Pcf11p in pre-mRNA 3′ end processing and in transcription termination. EMBO J. 2003; 22:2167–2177. [PubMed: 12727883]
21. Meinhart A, Cramer P. Recognition of RNA polymerase II carboxy-terminal domain by 3′-RNA-processing factors. Nature. 2004; 430:223–226. [PubMed: 15241417]
22. Krishnamurthy S, He X, Reyes-Reyes M, Moore C, Hampsey M. Ssu72 is an RNA polymerase II CTD phosphatase. Mol. Cell. 2004; 14:387–394. [PubMed: 15125841]
23. Meinhart A, Silberzahn T, Cramer P. The mRNA transcription/processing factor Ssu72 is a potential tyrosine phosphatase. J. Biol. Chem. 2003; 278:15917–15921. [PubMed: 12606538]
24. Nedea E, et al. Organization and function of APT, a subcomplex of the yeast cleavage and polyadenylation factor involved in the formation of mRNA and small nucleolar RNA 3′-ends. J. Biol. Chem. 2003; 278:33000–33010. [PubMed: 12819204]
25. Bataille AR, et al. A universal RNA polymerase II CTD cycle is orchestrated by complex interplays between kinase, phosphatase, and isomerase enzymes along genes. Mol. Cell. 2012; 45:158–170. [PubMed: 22284676]
26. Xiang K, et al. Crystal structure of the human symplekin-Ssu72-CTD phosphopeptide complex. Nature. 2010; 467:729–733. [PubMed: 20861839]
27. Nedea E, et al. The Glc7 phosphatase subunit of the cleavage and polyadenylation factor is essential for transcription termination on snoRNA genes. Mol. Cell. 2008; 29:577–587. [PubMed: 18342605]
28. Gilbert W, Guthrie C. The Glc7p nuclear phosphatase promotes mRNA export by facilitating association of Mex67p with mRNA. Mol. Cell. 2004; 13:201–212. [PubMed: 14759366]
29. He X, Moore C. Regulation of yeast mRNA 3′ end processing by phosphorylation. Mol. Cell. 2005; 19:619–629. [PubMed: 16137619]
30. Shi Y. Serine/threonine phosphatases: mechanism through structure. Cell. 2009; 139:468–484. [PubMed: 19879837]
31. Chu Y, Lee EY, Schlender KK. Activation of protein phosphatase 1. Formation of a metalloenzyme. J. Biol. Chem. 1996; 271:2574–2577. [PubMed: 8576223]

32. Egloff MP, Cohen PT, Reinemer P, Barford D. Crystal structure of the catalytic subunit of human protein phosphatase 1 and its complex with tungstate. J. Mol. Biol. 1995; 254:942–959. [PubMed: 7500362]
33. Haruki H, Nishikawa J, Laemmli UK. The anchor-away technique: rapid, conditional establishment of yeast mutant phenotypes. Mol. Cell. 2008; 31:925–932. [PubMed: 18922474]
34. Mayer A, et al. Uniform transitions of the general RNA polymerase II transcription complex. Nat. Struct. Mol. Biol. 2010; 17:1272–1278. [PubMed: 20818391]
35. Cho EJ, Kobor MS, Kim M, Greenblatt J, Buratowski S. Opposing effects of Ctk1 kinase and Fcp1 phosphatase at Ser 2 of the RNA polymerase II C-terminal domain. Genes Dev. 2001; 15:3319–3329. [PubMed: 11751637]
36. Peti W, Nairn AC, Page R. Structural basis for protein phosphatase 1 regulation and specificity. FEBS Journal. 2012; 280:596–611. [PubMed: 22284538]
37. MacKintosh C, et al. Further evidence that inhibitor-2 acts like a chaperone to fold PP1 into its native conformation. FEBS Lett. 1996; 397:235–238. [PubMed: 8955354]
38. Farkas I, Dombrádi V, Miskei M, Szabados L, Koncz C. Arabidopsis PPP family of serine/threonine phosphatases. Trends Plant Sci. 2007; 12:169–176. [PubMed: 17368080]
39. Kim T-W, et al. Brassinosteroid signal transduction from cell-surface receptor kinases to nuclear transcription factors. Nat. Cell Biol. 2009; 11:1254–1260. [PubMed: 19734888]
40. Chao Y, et al. Structure and mechanism of the phosphotyrosyl phosphatase activator. Mol. Cell. 2006; 23:535–546. [PubMed: 16916641]
41. Kim M, et al. The yeast Rat1 exonuclease promotes transcription termination by RNA polymerase II. Nature. 2004; 432:517–522. [PubMed: 15565157]
42. Logan J, Falck-Pedersen E, Darnell JE, Shenk T. A poly(A) addition site and a downstream termination region are required for efficient cessation of transcription by RNA polymerase II in the mouse beta maj-globin gene. Proc. Natl. Acad. Sci. U.S.A. 1987; 84:8306–8310. [PubMed: 3479794]
43. Mischo HE, Proudfoot NJ. Disengaging polymerase: Terminating RNA polymerase II transcription in budding yeast. Biochim. Biophys. Acta. 2013; 1829:174–185. [PubMed: 23085255]

METHODS REFERENCES

44. Passmore LA, et al. Doc1 mediates the activity of the anaphase-promoting complex by contributing to substrate recognition. EMBO J. 2003; 22:786–796. [PubMed: 12574115]
45. Sydow JF, et al. Structural basis of transcription: mismatch-specific fidelity mechanisms and paused RNA polymerase II with frayed RNA. Mol. Cell. 2009; 34:710–721. [PubMed: 19560423]
46. Chapman RD, et al. Transcribing RNA polymerase II is phosphorylated at CTD residue serine-7. Science. 2007; 318:1780–1782. [PubMed: 18079404]
47. Mayer A, et al. The spt5 C-terminal region recruits yeast 3′ RNA cleavage factor I. Mol. Cell. Biol. 2012; 32:1321–1331. [PubMed: 22290438]
48. Nagalakshmi U, et al. The transcriptional landscape of the yeast genome defined by RNA sequencing. Science. 2008; 320:1344–1349. [PubMed: 18451266]

Europe PMC Funders Author Manuscripts

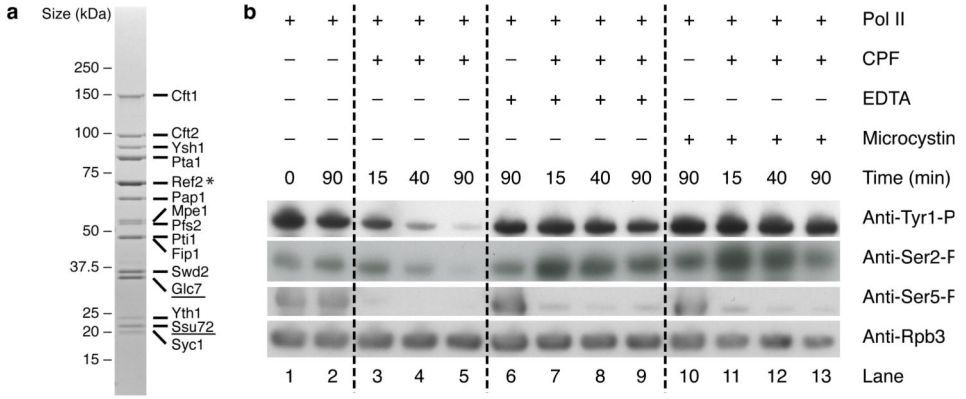

Figure 1.

CPF subunit Glc7 is a Pol II CTD Tyr1 phosphatase *in vitro*. (**a**) SDS-PAGE analysis of purified yeast CPF. An asterisk marks the tagged protein Ref2; the phosphatases Ssu72 and Glc7 are underlined. Identities of bands confirmed by mass-spectrometry are labeled. (**b**) *In vitro* dephosphorylation assay measuring CPF activity towards phosphorylated Pol II CTD as shown by Western blotting with antibodies against Pol II subunit Rpb3 and Tyr1-phosphorylated (Tyr1-P), Ser2-P and Ser5-P CTD residues (1Y26, 3D12, 3E10 and 3E8 antibodies, respectively). For lanes 6–13, 10 mM EDTA or 200 nM microcystin were included in the reactions. Uncropped versions of blots can be found in Supplementary Fig. 4a.

Europe PMC Funders Author Manuscripts

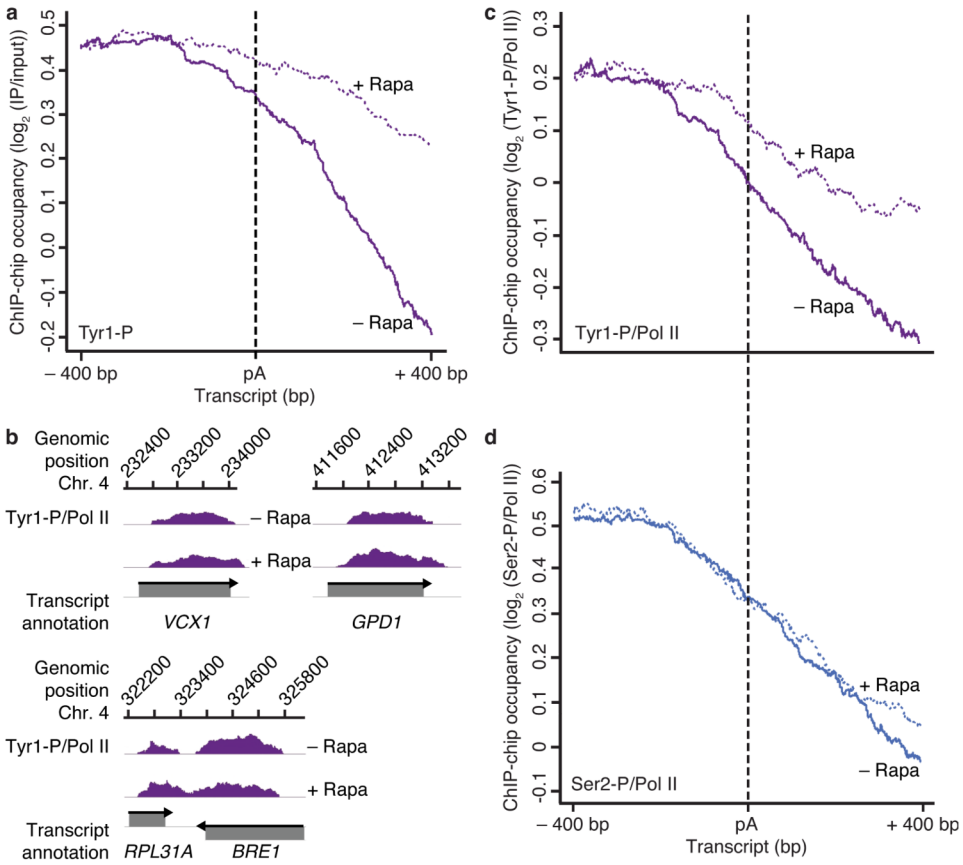

Figure 2.

Glc7 is required for Tyr1 but not Ser2 dephosphorylation *in vivo*. (**a**) Metagene analysis for genome-wide ChIP occupancy of Tyr1-phosphorylated Pol II around polyA (pA) sites in the Glc7 anchor-away strain, treated with rapamycin to deplete Glc7 from the nucleus (+ Rapa, violet dotted line) or untreated (− Rapa, violet solid line). Averaged ChIP-chip signals are plotted as the median signal ($\log_2$ (IP/input)) at each genomic position over a set of 619 representative genes (Online Methods), normalized to have approximately equal occupancy levels upstream (around −400 bp) of the pA site (dashed black line). The profiles are shown from 400 nucleotides upstream to 400 nucleotides downstream of the pA site. Non-normalized data averaged over the entire gene length are shown in Supplementary Fig. 2. Experiments were performed in biological duplicates. (**b**) Profiles of Tyr1-P levels normalized to total Pol II (Fig. 4a) on selected genes, smoothed by a 150 nt window running median are shown in purple. Below, grey boxes indicate transcripts on the Watson (top) and Crick strands (bottom). (**c,d**) ChIP-chip occupancy profiles of Tyr1- (**c**) and Ser2- (**d**) phosphorylated Pol II over 619 genes aligned at the pA site (dashed line) and normalized against the corresponding Rpb3-profile (Fig. 4a) without and with rapamycin (solid and dotted lines, respectively). Experiments were performed in biological duplicates.

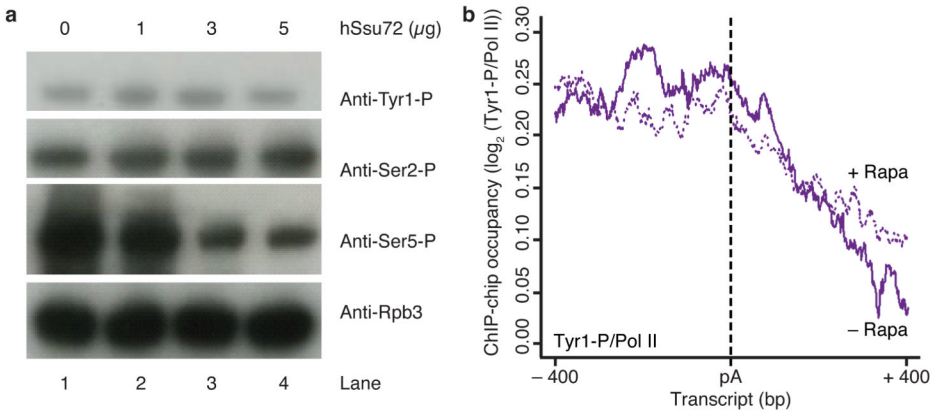

Figure 3.

Ssu72 does not change Tyr1 phosphorylation levels *in vitro* and *in vivo*. (**a**) *In vitro* dephosphorylation assay of Pol II CTD with recombinant human Ssu72, monitored by Western blotting with antibodies against Pol II subunit Rpb3 and Tyr1-phosphorylated (Tyr1-P), Ser2-P and Ser5-P CTD residues (1Y26, 3D12, 3E10 and 3E8 antibodies, respectively). Uncropped versions of blots can be found in Supplementary Fig. 4b. (**b**) ChIP-chip occupancy profiling of Tyr1-phosphorylated Pol II over 619 genes aligned at the pA site (dashed line) and normalized against the corresponding Rpb3 profile without and with rapamycin treatment (solid and dotted lines, respectively) in a Ssu72 anchor away strain. Profiles in a region from 400 nucleotides upstream to 400 nucleotides downstream of the pA site are shown. This experiment was performed in biological duplicate.

Europe PMC Funders Author Manuscripts

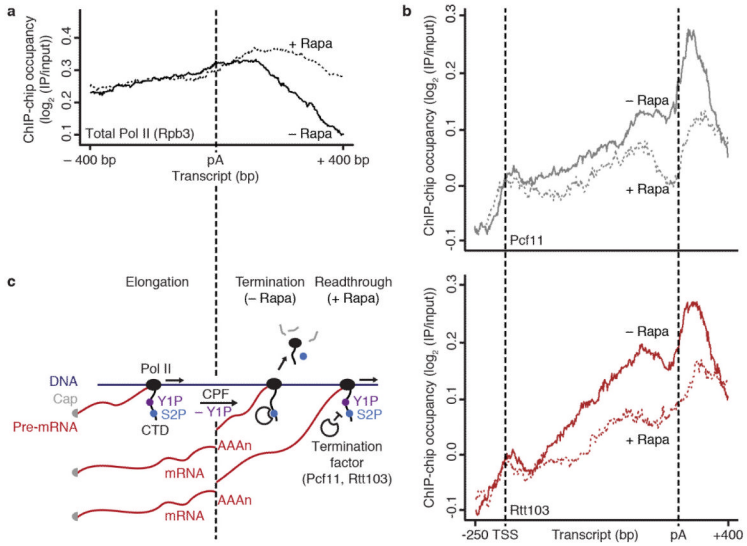

Figure 4.

Tyr1 dephosphorylation by Glc7 is required for normal termination factor recruitment and transcription termination *in vivo*. (**a**) Metagene analysis for genome-wide ChIP occupancy of total Pol II (subunit Rpb3) around polyA (pA) sites in the Glc7 anchor-away strain with rapamycin treatment (+ Rapa, black dotted line) and untreated (− Rapa, black line). Averaged ChIP-chip signals are shown as the median signal ($\log_2$ (IP/input)) at each genomic position over a set of 619 representative genes (Online Methods) and normalized to have approximately equal occupancy levels upstream (around −400 bp) of the pA site. (**b**) ChIP-chip occupancy profiling of TAP-tagged Pcf11 (top) and Rtt103 (bottom) in the Glc7 anchor-away strain, after treatment with rapamycin (+ Rapa, dotted lines) and untreated (− Rapa, solid lines). The profiles show ChIP-chip signals averaged by taking the median signal ($\log_2$ (IP/input)) at each genomic position over a set of representative medium length genes (1238 ± 300 bp, n = 339, Online Methods). TSS, transcription start site. Experiments in (**a**,**b**) were performed in biological duplicates. (**c**) Model for the Pol II elongation-termination transition. DNA is dark blue, RNA is dark red, Pol II and its CTD are black; Ser2-P is blue and Tyr1-P is purple. For details see within text.

Europe PMC Funders Author Manuscripts